J Mater Sci: Mater Electron (2007) 18:S61–S64
DOI 10.1007/s10854-007-9174-z

Optical devices from porous silicon having continuously varying refractive index

S. Ilyas · M. Gal

Published online: 20 March 2007

Abstract We shall discuss two types of optical devices made using porous silicon, in which the refractive index distribution is continuous. In the rugate filter, the refractive index profiles is sinusoidal along the growth axis, while in the graded refractive index lenses that we fabricated from PSi, the refractive index is quadratic in the plane of the porous layer. We shall talk about the design and fabrication methods used to manufacture both of these device types, and show examples for each.

1 Introduction

Even though porous silicon (PSi) has been known for almost 50 years, there has been an upsurge of interest in this unusual material. The first reports giving details of a new form of silicon appeared in 1956 when Uhlir [1] described a study of the electro-polishing of silicon in hydrofluoric acid. Activity in PSi increased significantly after 1990 when efficient visible luminescence was discovered by Canham [2] suggesting the possibility of silicon based light sources. However, in spite of considerable research effort during the subsequent years, stable, efficient and reproducible electroluminescence could not be achieved. On the other hand, the intensive research has resulted in numerous and often unforeseen applications that rely on other valuable properties of PSi, such as its large surface area and bio-compatibility, and its ''made to order'' refractive index [3]. Emerging applications now cover a broad spectrum of fields, from chemical and biomedical sensing to microelectronics and micro-electromechanical system (MEMS), as well as a range of optical and optoelectronic applications.

During the last decade or so, several types of optical devices have been made from PSi, including laser mirrors, micro-cavities, filters, etc. These devices are similar to conventional optical devices in that they use alternate layers of high and low refractive index material. In this article, we shall concentrate on two types of optical devices, the rugate filters and gradient refractive index (GRIN) lenses, both of which are based on *continuously* varying refractive index distributions in the PSi.

2 Rugate filters

Rugate filters are a type of optical filters that contain a *continuous* variation of the refractive index, usually sinusoidal, along the growth axis [4–6]. The reflectance spectrum of such a filter shows a high reflectivity ''stop-band'' around a characteristic wavelength, λ_0, and very low reflectivity elsewhere. Rugate filters, first developed by Berger et al. [7] and Lorenzo et al. [8], are often preferred over conventional step-index multilayer filters because they do not display higher order harmonics. Filters reported so far had relatively broad stop-bands, usually of the order of several hundred nanometres. While large stop-bands are adequate or even desirable in some applications, we were interested in narrow line-width rugate filters for sensor applications, and hence developed filters with very narrow linewidths. In this study, therefore we shall describe our approach and results in making narrow line-width rugate filters.

S. Ilyas · M. Gal (✉)
School of Physics, The University of New South Wales, Sydney 2051, Australia
e-mail: m.gal@unsw.edu.au

Rugate filters are made by sinusoidally varying the refractive index of the material along the growth axis. The refractive index profile, $n(x)$, of a rugate filter centred on λ_0 can be written in the following form:

$$n(x) = n_0 + \Delta n/2 \sin(4\pi x/\lambda_0) \quad (1)$$

where x is the perpendicular distance into the plane of the filter, n_0 is the average refractive index, and Δn is the refractive index contrast[9]. Such a sinusoidal profile would result in the reflection spectrum displaying a single stop-band at λ_0, the bandwidth of which depends on the magnitude of Δn. However, because of the sharp truncation of the refractive index modulation at the boundaries of the filter, such a simple sinusoidal index profile would also generate interference oscillations appearing on both sides of the stop-band (''side lobes''). To suppress these unnecessary oscillations, the abrupt termination of the index profile has to be faded out or *apodized* with a smooth envelope function so as to reduce the index contrast to zero at the boundaries. In our filters, we used a Gaussian function as the envelope to the sinusoidal refractive index which resulted in the reduction of the side lobes while at the same time not influencing the optical properties of the stop-band. To further reduce interference oscillations resulting from the refractive index mismatch between the average index of the filter and the surrounding media, we grew additional continuously varying so called ''index matching'' layers that aimed to match the refractive indexes of the surface and the substrate to the filter.

A graphical illustration of the overall refractive index profile is shown in Fig. 1, and includes an amplitude modulated sinusoidal refractive index apodized with a Gaussian function, and two 3rd order polynomial index matching layers at the front and substrate end of the filter. In the example to be discussed below, the filter included 40 sinusoidal periods with an index contrast of $\Delta n = 0.028$ ($n_{HI} = 2.122$ and $n_{LO} = 2.094$). The index matching layer at the surface was designed to have a thickness of 450 nm, and the refractive index that smoothly decreased from 2.094 to 1.471 (which is the lowest refractive index value we could achieve). The index matching layer at the Si substrate side was 675 nm thick, and the refractive index increased from $n = 2.094$ to $n = 3.5$ as a 3rd order polynomial.

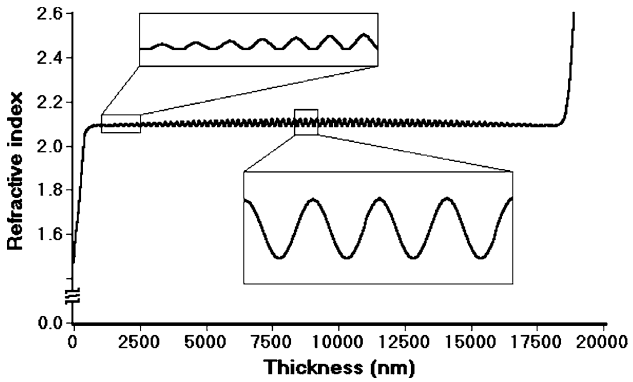

Fig. 1 Refractive index distribution of our rugate filters, having amplitude modulated (apodized) sinusoidal refractive index with index matching layers at the front and the substrate end of the filter to match air and the Si substrate, respectively. The inserts show the apodization of the index, and the sinusoidal variation as a function of depth

The reflectivity spectrum of a filter having an index profile shown in Fig. 1 was calculated using the characteristic matrix method [10, 11], and is shown in Fig. 2. As can be seen, the chosen conditions lead to a stop-band at 850 nm with a FWHM of approximately 5 nm, and a maximum reflectivity of 65%. The reflectivity outside the stop-band is calculated to be less than 10%.

After designing the filters, we used standard electrochemical etch to fabricate the PSi rugate filters into Si wafers [12] in accordance with the simulation parameters. The filters described above were prepared from highly boron doped p^+-type (100) silicon wafers having a resistivity of 0.07 ohm cm. The Si substrate was electrochemically etched at room temperature in a solution of 25% HF. This etching solution was prepared by diluting 48% HF solution into ethanol. We used Keithley 2400 SourceMeter® to generate a computer-controlled sinusoidal current profile for the electrochemical etching process. The current profile, which includes the index matching and the apodization functions, is generated by a small program based on

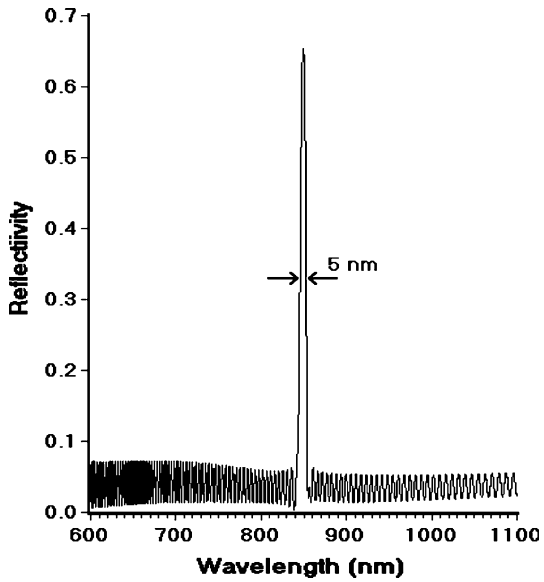

Fig. 2 Calculated reflectivity spectrum of a rugate filter assuming 40 sinusoidally varying refractive index layers, Gaussian apodization and index matching layers at the surface and substrate ends

LabVIEW 6.1. The current density for producing the sinusoidal porosity is 2.205 to 2.256 mA/mm^2. During the etching process temporal breaks of 9 s were used at each sinusoidal period during the anodization to recover the HF concentration at the dissolution front. After the etching process, the samples were rinsed with ethanol. We used pentane drying to minimize the effects of capillary pressure within the porous structure.

The measured reflectivity spectrum of the filter discussed in this publication is shown in Fig. 3. The reflectivity was measured by illuminating the sample at normal incidence with monochromatic light from a J/Y SPEX 1681 0.22 m spectrometer and measuring the reflected beam with a silicon detector. The measurement was taken over an area of 0.5 mm^2 on the surface, and the collecting angle was 2.7^0. As can be seen, the agreement between the calculated and measured spectra is good. The measured spectrum has a stop-band at 848 nm (850 nm was predicted by the theory), maximum reflectivity 63% (65% predicted), and line-width of 11 nm (5 nm was predicted). The line-width is slightly broader than the theoretically predicted linewidth due to the large collection angle used in the reflectivity measurements. The reflectivity outside the stop-band is less than 10%. These types of filters are currently being used in biochemical sensing projects[13].

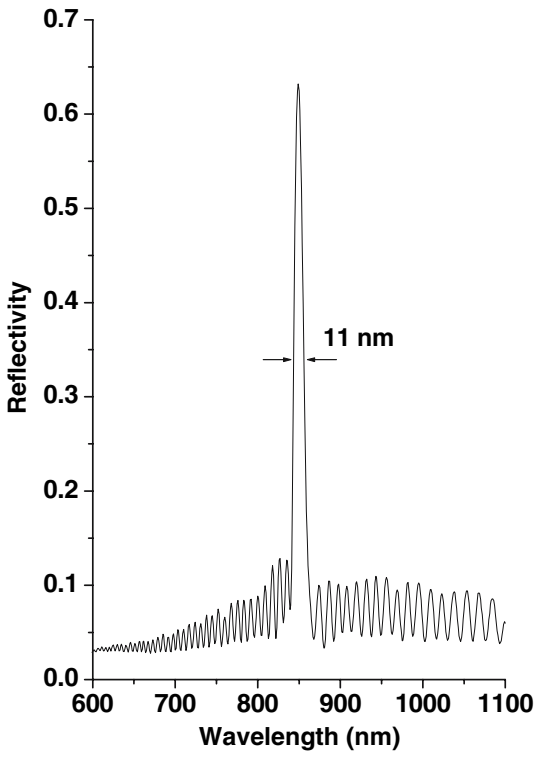

Fig. 3 Measured reflectivity spectrum of a rugate filter having a refractive index profile shown in Fig 1

3 GRIN lenses

Graded refractive index (GRIN) devices have continuous variation of refractive index in the direction perpendicular to the growth direction[14]. Such radial refractive index gradient devices are well known and are routinely fabricated from glasses and plastics, and are commonly used as (GRIN) lenses[15]. Advantages of PSi based GRIN lenses include their compatibility with Si optoelectronics, and hence their possible integration with other Si devices, and their transparency from the visible to the infrared part of the spectrum, including the optical communications window between $1.3\ \mu m < \lambda < 1.6\ \mu m$. Since the refractive index of PSi is proportional to the porosity of the material, when making a GRIN lens our aim was to achieve a specific circularly symmetric porosity distribution with a nearly quadratic distribution of the optical thickness (the product of the refractive index and the physical thickness) as a function of the radial distance from the optical axis:

$$N_{\mathrm{ot}}^2(r) = [n(r)L(r)]^2 = N(0)^2(1-\alpha^2 r^2) \tag{2}$$

Here n is the refractive index and L is the thickness of the layer. This means that the (etching) current density has to be maximum in the centre of the sample and has to decrease continuously towards the edge of the sample. To achieve such a current density, we replaced the disk electrode (anode) in the electrochemical cell with one that only touches the (back of the) Si wafer in the shape of an outer ring. Such a ring electrode will result in an optical thickness with the required profile for the formation of GRIN lens [16].

Using such a ring electrode, the effective current distribution in the silicon wafer is:

$$j_e = 2\sqrt{\frac{c^2(d^2+R^2+r^2)}{(d^2+(R-r)^2)(d^2+(R+r)^2)}} \tag{3}$$

where c is a constant which depends on the resistivity of the silicon and the current applied to the wafer, R is the radius of the Si (i.e. the PSi area), and d is the thickness of the wafer. It can be shown[14] that such a current distribution will produce an optical thickness distribution given by:

$$OPT = b_1 - b_2\sqrt{\frac{c^2(d^2+R^2+r^2)}{d^4+(R^2-r^2)^2+2d^2(R^2+r^2)}} - \frac{b_3c^2(d^2+R^2+r^2)}{d^4+(R^2-r^2)^2+2d^2(R^2+r^2)} \tag{4}$$

where b_1, b_2, and b_3 are constants.

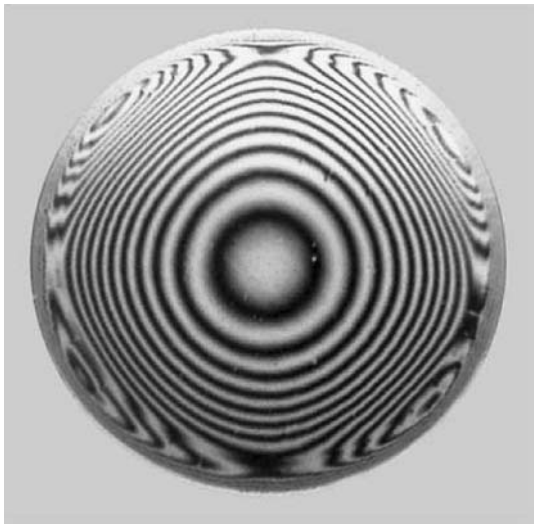

Fig. 4 PSi samples with lateral variation in refractive index under illumination with monochromatic light. The ring shows the continuous change in the optical thickness from the centre to the edge

Since the optical thickness (Eq. 4) depends on the resistivity of the wafer through the parameter '*c*', we made a number of different lenses using silicon wafers with different resistivities: 0.05, 0.2, and 2.0 ohm cm. The electrochemical etching was performed with ethanoic hydrofluoric acid with 25, 30 and 35% HF at room temperature.

Figure 4 shows an interferogram of a PSi GRIN lens illuminated with a sodium lamp. The interference patterns (also called Newton's rings) clearly show the radially varying optical thickness. Using the interferogram, we can calculate the optical thickness distribution of the PSi film as a function of the radius. The optical thickness of the PSi layer shown in Fig. 4 as a function of the radial distance is shown as the dark squares in Fig. 5. Also shown on this figure is the quadratic dependence (solid line) and the plot of Eq. (4), the theoretically expected position dependence for a GRIN lens. As can be seen, there is excellent agreement between the experiment and theory.

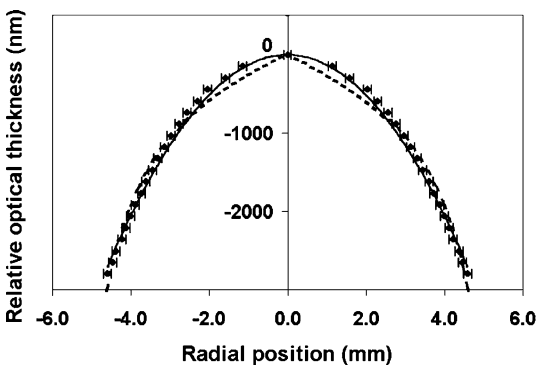

Fig. 5 Relative optical thickness of PSi samples as function of the radius. The data points with error bars represent the experimentally determined relative optical thickness of a 10 mm diameter GRIN lens versus radial distance. The full line is the best fit to the experimental data assuming quadratic position dependence, as required by a GRIN lens equation (Eq.(1)). The dashed line represents the calculated optical thickness (Eq. (4))

4 Conclusion

We have designed, fabricated and tested rugate filters and GRIN lenses made using PSi. In both these types of devices the refractive index distribution is continuous.

References

1. A. Uhlir, Bell System Tech. J, **35**, 333 (1956)
2. L.T. Canham, Appl. Phys. Lett.**57**, 1046 (1990)
3. O.Bisi, S. Ossicini, L. Pavesi, Surf. Sci. Rep. **38**, 1–126 (2000)
4. B.G. Bovard, Appl. Opt. **32**, 28 (1993)
5. J. Volk, M. Fried, A.L. Toth, I. Barsony, Thin Solid Films **455**(456), 535–539 (2004)
6. N. Perelman, I. Averbukh, J. Appl. Phys. **79**, 6 (1996)
7. M.G. Berger, R. Arens-Fischer, M. Thönissen, M. Krüger, S. Billat, H. Lüth, S. Hilbrich, W. Theiß, P. Grosse, Thin Solid Films **297**, 237 (1997)
8. E. Lorenzo, C.J. Oton, N.E. Capuj, M. Ghulinyan, D.N. Urrios, Z. Gaburro, L. Pavesi. Phys. Stat. Sol. (c). **2**(9), 3227–3231(2005)
9. S. Ilyas, T.Böcking, K. Kilian, P.J. Reece, J. Gooding, K. Gaus and M. Gal, Opt. Mat. **29**, 619–622 (2007)
10. G.T. Dalakos, *Computer Simulation of Rugate Optical Interference Filters by Using the Characteristic Matrix Method I: Introduction and Simple Application*, (General Electric Research and Development Center, 1999)
11. H.S. Nalwa, *Handbook of Thin Film Materials Ferroelectric and Dielectric Thin Films*, vol.3, (Academic Press, San Diego, CA, 2002)
12. A. Bruyant, G. Lerondel, P.J. Reece, M. Gal. Appl. Phys. Lett. **82**, 227 (2003)
13. T.Böcking, K.A. Kilian, T. Hanley, S. Ilyas, K. Gaus, M. Gal, and J.J. Gooding, Langmuir, **21**, 10522–10529 (2005). B.E.A. Saleh, M.C. Teich, *Fundamental of Photonics*, (John Wiley & Sons, Inc, New York, 1991) p. 23
14. B.E.A. Saleh, M.C. Teich. *Fundamental of Photonics*, (John Wiley & Sons, New York , 1991) p. 23
15. A.D.Pearson, W.G. French, E.G. Rawson in *Selected Papers on Gradient-index Optics*, ed. by D.T. Moore. SPIE Milestone Series, MS67. (1993) p. 193
16. S. Ilyas and M. Gal, Gradient refractive index planar microlens in Si using porous silicon (to be published)